ELSEVIER

Polymer 42 (2001) 5893–5899

polymer

www.elsevier.nl/locate/polymer

Lamellar characteristics controlled by prior polymer concentration for solution-crystallized ultra-high molecular weight polyethylene

H. Uehara*, H. Matsuda, T. Aoike, T. Yamanobe, T. Komoto

Department of Chemistry, Gunma University, Kiryu, Gunma 376-8515, Japan

Received 1 May 2000; received in revised form 15 October 2000; accepted 6 December 2000

Abstract

The effect of prior polymer concentration on solution-crystallized morphologies in ultra-high molecular weight polyethylene has been characterized by transmission electron microscopy (TEM) and X-ray analysis. Molecular motion in crystalline and amorphous phases was evaluated by nuclear magnetic resonance (NMR) techniques. The series of solution-crystallized mats was prepared from different polymer concentrations. TEM results indicate these samples consist of lamellae aligned parallel to the mat surface. The observed high order scattering of small-angle X-ray scattering (SAXS) patterns indicate a regular stacking of lamellae. The long period was ~11 nm, independent of prior polymer concentration. Wide-angle X-ray diffraction analysis also revealed the same level of crystallinity for these solution-crystallized samples, well coincident with ^{1}H-NMR results. These indicate that the thickness of crystal/amorphous layers was constant, which was also confirmed by layer thickness distribution analysis for this series of samples, based on direct TEM observation. However, the SAXS peak gradually grew and sharpened with increasing prior polymer concentration. ^{1}H-NMR results also indicate amorphous chain mobility was restricted for the sample prepared from lower polymer concentration in spite of unchanged crystallinity and relaxation characteristics for crystalline chains. Morphological and relaxation characteristics information demonstrates that lower prior polymer concentration might prefer formation of tie molecules which connect tightly crystalline layers. In contrast, the higher concentration could trap loosely entangled chains in amorphous layers, providing for an ease of chain relaxation estimated by ^{1}H-NMR analysis. © 2001 Published by Elsevier Science Ltd.

Keywords: Entanglements; Tie molecules; Ultra-high molecular weight polyethylene

1. Introduction

The elusive concept of 'polymer entanglements' has been the subject of conjecture for some 50 years. Even though there may be no direct experimental observation, a mountain of indirect evidence and consistent logic has led to the general acceptance of entanglements, and even their quantities and dependence on polymer concentration in solution.

The first evaluation of chain entanglement for polyethylene (PE) was offered by Porter and Johnson [1]. They showed that the molecular weight (MW) dependence of melt-viscosity changed at a critical MW. Similar abrupt viscosity changes were observed in plots of polymer concentration versus solution viscosity in poor solvents [2]. It was concluded that: (i) above this critical polymer concentration (ϕ_c), entanglements develop in the polymer solution, and (ii) below this ϕ_c, the chains are essentially isolated.

The existence of entanglements in the solid state has been experimentally proved only by sample drawability. Smith et al. [3] reported that the drawability of pure ultra-high molecular weight polyethylene (UHMW-PE) is significantly affected by the prior polymer concentration for the preparation of gels. This tendency was well interpreted by entanglement concepts. Assuming that the entanglements in solution are essentially retained, both on sample crystallization and solid-state drawing, a lower entanglement density in the dilute solution for gel formation is considered the reason for their higher drawability. Similar results have been reported for other semi-crystalline polymers [4].

These conclusions suggest that even high MW chains can be well extended on draw of non-entangled samples. In fact, UHMW-PE single crystal mats containing few entanglements have been effectively super-drawn up to a maximum draw ratio of 300 by two-stage draw [5]. Such highly drawn films exhibit a tensile modulus of 220 GPa, a value approaching the chain-axis crystal modulus of PE determined by X-ray diffraction (240 GPa [6]).

For semi-crystalline polymers, including PE, such

* Corresponding author. Tel.: +81-277-30-1332; fax: +81-277-30-1333.
E-mail address: uehara@chem.gunma-u.ac.jp (H. Uehara).

0032-3861/01/$ - see front matter © 2001 Published by Elsevier Science Ltd.
PII: S0032-3861(00)00911-3

entanglements are segregated into the amorphous region during solution-crystallization with regular chain folding on lamellar surfaces. Thus, these entanglement characteristics can be expected to depend on their prior ϕ. However, such a systematic study of entanglement formation has not been previously reported for PE, except for the drawability data [3].

For amorphous polymers, evaluation of entanglements in the solid state has been accomplished by neutron scattering measurements. Based on such measurements, using deuterium-labeled chains, Higgins and Stein [7] assert that the radius of random coils in a theta solution of atactic polystyrene is identical to that of amorphous chains in the solid-state. This means that the MW between entanglements in the amorphous region is identical to the solid and theta states. Also, Porter and co-workers [8] examined neutron scattering on drawing of deuterium-labeled polystyrene. They reported that the molecular draw ratios determined by the neutron scattering measurements is coincident with the macroscopic draw ratios, corresponding to an 'affine deformation'. This suggests that the disentanglement of polystyrene chains does not occur on drawing, consistent with the above assumption by Smith et al. [3] for PE chain entanglements.

Recently, the neutron scattering technique has been successfully applied to crystallization analysis for solid PE by Sasaki et al. [9]. They selected the miscible combination of hydrogenated low-density PE having short branches and deuterium-labeled linear PE. It was concluded that the radius of the random coils of deuterium-labeled linear PE in the melts can be kept even in crystallized morphology, which is quite similar to the neutron scattering results for amorphous polystyrene in the molten and solution states. Here, the miscibility between deuterium-labeled and regular chains can sometimes be a key for better reliability on interpretation of neutron scattering results. For semi-crystalline polymers, separated crystallization of each labeled and regular chain provides their individual lamellar formation, due to their different thermal properties (for example, melting temperatures). Unfortunately, for a set of deuterium-labeled and usual hydrogenated linear PE chains, their actual immiscibility still limits an ideal analysis of random distribution of these chains in the same lamella.

Nuclear magnetic resonance (NMR) analysis has the distinct advantage of separated evaluations for crystalline and amorphous chain motions. We have reported that the molecular chain mobility change during heating of UHMW-PE samples can be successfully interpreted through ^{1}H-NMR relaxation analysis, assuming an appropriate combination of several decay functions [10]. This technique provides a rare opportunity to characterize amorphous chains. These data, combined with results obtained by other methods such as X-ray measurements and electron microscopy, may provide a better understanding of structural characteristics of both crystalline and amorphous regions.

Many ^{1}H-NMR analyses have been performed for the molten or solution state of PE to characterize random coiled molecular chains [11–20]. In contrast, the relaxation evaluation for solid-state amorphous PE chains remains ambiguous because crystallization emphasizes the rigid component having a beating profile [10]. Therefore, the difficulties of free induction decay (FID) resolution are sometimes introduced. Cohen-Addan et al. [20] have measured the ^{1}H-NMR relaxation for swollen PE gels obtained by quenching semi-dilute solution. However, the contained solvent obscures the polymer concentration effects on entanglement formation in the amorphous phase.

The purpose of the present study is to evaluate the effects of prior polymer concentration on amorphous chain characteristics. A combination of several analytical techniques are employed and the results are interpreted according to the above entanglement concept. Another major restricted state of amorphous chains would be 'tie molecules' which lie between crystals. UHMW characteristics could eliminate chain end effects on structural formation of amorphous phases in solution-crystallized morphology.

2. Experimental

2.1. Sample preparation

Hifax 1900 from Montel, the highly linear UHMW-PE utilized, has a viscosity average MW of 4×10^6. To obtain samples in a reduced entangled state, a 0.05 wt% dilute tetralin solution of UHMW-PE with 0.1 wt% (based on polymer) antioxidant of 2,6-di-*tert*-butyl-*p*-cresol was prepared at boiling point under a nitrogen gas flow. The higher dissolution temperature in tetralin was preferred for possible diffusion of PE molecular coils in the solution. The tetralin solutions were quenched into ice water to capture the reduced entangled state. The single crystal-like aggregates were filtered into mats at room temperature (RT). The obtained solution-grown crystal (SGC) mat was well dried at RT in vacuo. Other crystalline mats were also prepared from 0.1 to 0.5 wt% tetralin solution by the same procedure.

2.2. Measurements

Small-angle X-ray scattering (SAXS) patterns were recorded on a Rigaku type small-angle vacuum camera and imaging plate system. Cu-Kα radiation was generated at 40 kV and 150 mA by a Rigaku Type RU-200 rotating anode X-ray generator. An imaging plate pattern was recorded with the incident beam parallel to the mat surface. The exposure time was always 3 h. Scattering diagrams were reduced from the imaging plate patterns using a Rigaku type *R*-axis reading system. Wide-angle X-ray diffraction (WAXD) patterns were also recorded by a Rigaku type diffractometer system RAD-IIIA equipped with a sealed tube type X-ray generator operated at 40 kV and 25 mA. All X-ray measurements were made with

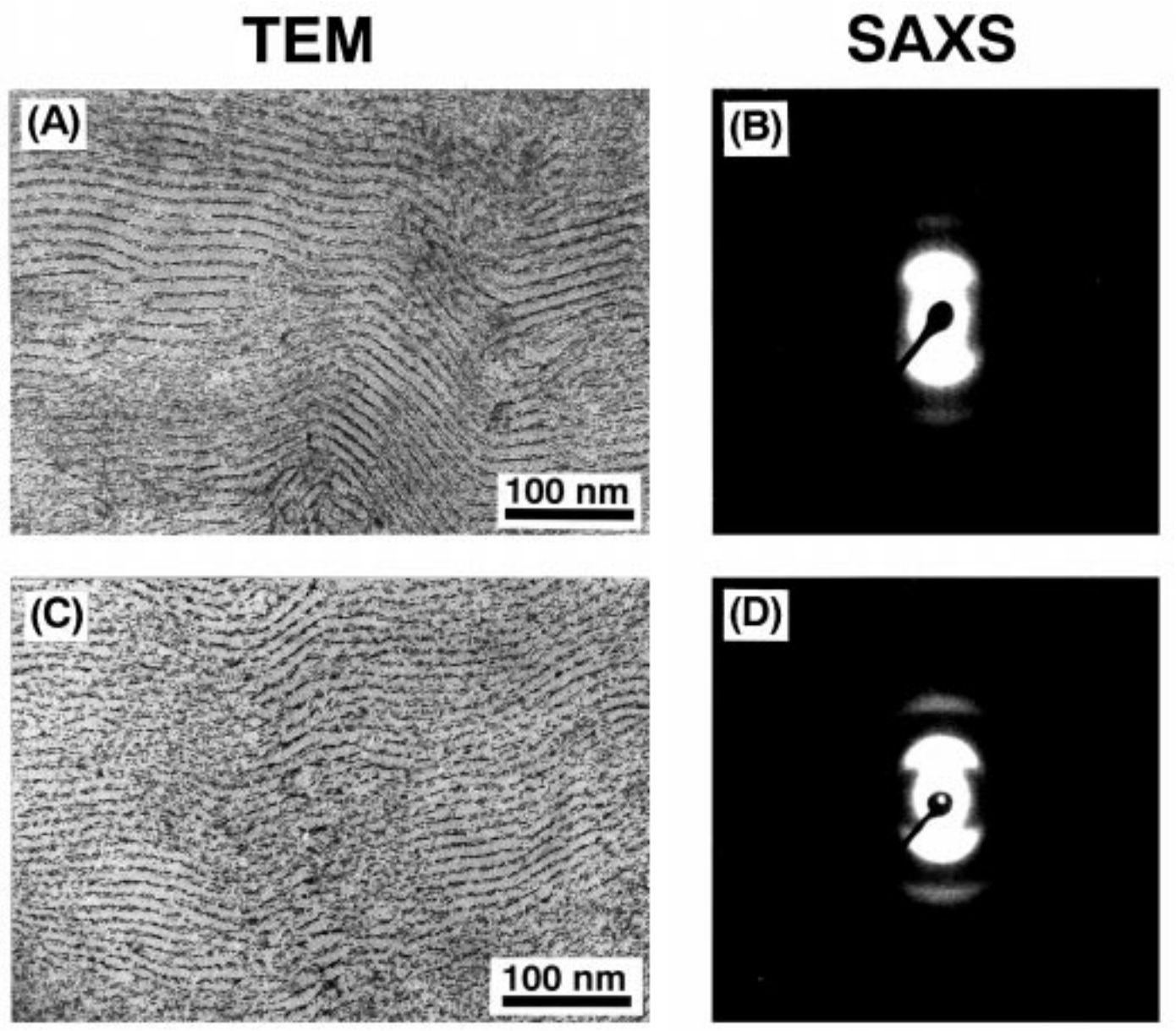

Fig. 1. Two sets of TEM and SAXS patterns viewed parallel to the wide surface of a mat precipitated from: (A, B) 0.05; and (C, D) 0.2 wt% tetralin solution. The mat surface was arranged horizontally in this figure.

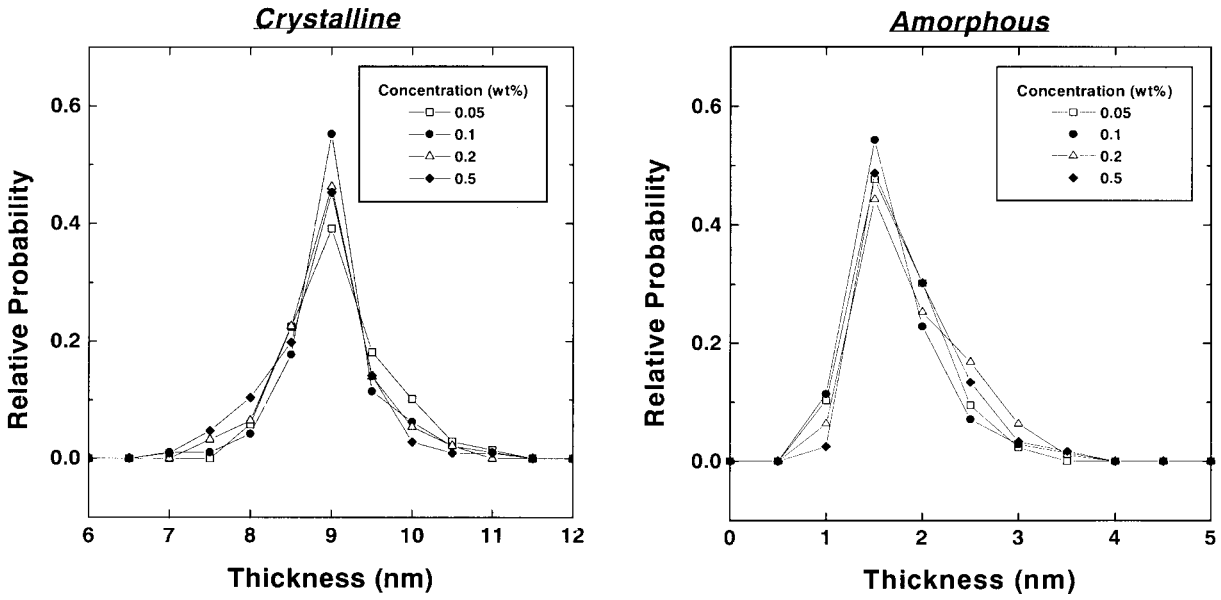

Fig. 2. Two sets of thickness distribution curves for crystalline (left) and amorphous layers (right), estimated from TEM images.

Cu-Kα radiation monochromatized with a graphite monochrometer.

Transmission electron microscopy (TEM) observations were obtained by a JEOL 1200EMX electron microscope operated at 80 kV. The samples were stained by RuO_4 vapor and embedded in epoxy resin. The assembly was cut into thin sections 60 nm thick using a Reichert UltraCut S. microtome for TEM observation.

^{1}H-NMR measurements were carried out at RT with a JEOL MU-25 solid-state pulse NMR spectrometer equipped with a 25 MHz magnetic field. The FID was recorded by the solid-echo method. Data was collected every 0.2 μs. The dead time before signal sampling was 2 μs. To eliminate effects of chain orientation towards the magnetic field on spectrum shape, sample mats were cut into 1 mm^2 size and randomly packed in a sample tube.

3. Results and discussion

3.1. Solution-crystallized morphology

TEM observations and X-ray measurements were conducted to clarify the crystalline morphology of SGC mats precipitated from 0.05 to 0.5 wt% tetralin solution. Fig. 1 presents typical TEM images viewed from the edge of the mat and SAXS patterns obtained with the incident beam parallel to the mat surface for two samples prepared from prior polymer concentrations of 0.05 and 0.2 wt%. For all images obtained by both TEM and SAXS, the sample mat was placed along the horizontal direction. The SAXS pattern of the mat indicated lamellae oriented parallel to the mat surface for both samples and was essentially the same for all other samples precipitated from 0.1 and 0.5 wt% solution. These results also reveal that the crystalline chains were oriented perpendicular to the surface of the initial mat. A combination of WAXD patterns obtained with the incident beam both parallel and perpendicular to the mat surface for the series of solution-crystallized samples also supports the chain orientation assignment. Further, even third-order scattering peaks could be clearly observed in the SAXS pattern for all solution-crystallized samples prepared in this study. Each lamella has an identifiable thickness and the lamellae are stacked regularly, even for a higher polymer concentration of 0.5 wt% at prior solution-crystallization. Lamellar thickness estimated from long periods in SAXS patterns was ~11.5 nm, independent of prior polymer concentration. A detailed value determination of the long period was examined by scattering diagrams reduced along the horizontal direction in imaging plate patterns, described later.

TEM observation results revealed the regular stacking of crystalline lamellae in all of solution-crystallized mats, which has been predicted from above SAXS data interpretation. As shown in Fig. 1(A) and (C), these crystalline lamellae are alternatively sandwiched with dark layers indicating amorphous region. From low magnification images (not shown here), it was also found that such a lamellar structure expanded laterally through several-μm length. It should be noted that these morphological characteristics of lamellar stacking and orientation were common for all SGC mats. The lamellar thickness corresponding to SAXS long period could be defined as a set of crystal and amorphous layer thickness in these TEM images, which was always ~11 nm for all solution-crystallized mats prepared at different prior polymer concentrations.

One of the benefits of direct TEM observation results is its possible accounting for the thickness of crystalline/

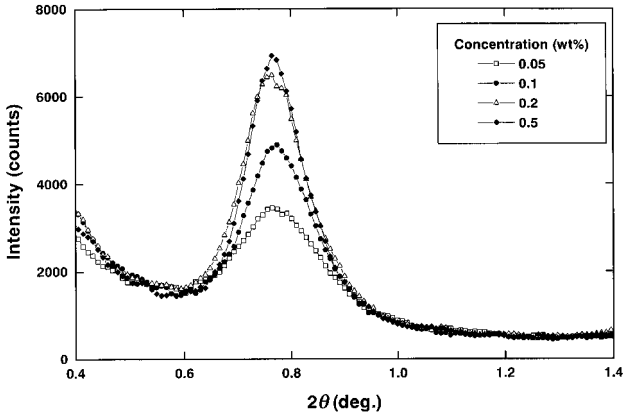

Fig. 3. SAXS intensity profile for the series of samples solution-crystallized from 0.05 to 0.5 wt% tetralin solution. The background was subtracted from original data plots.

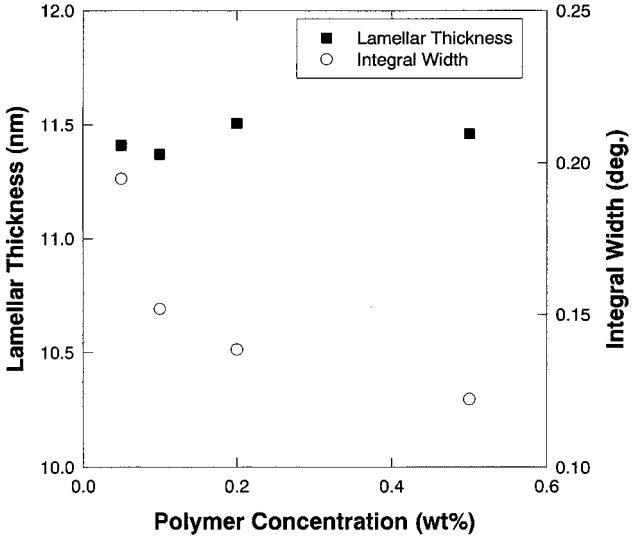

Fig. 4. The long period and integral width of SAXS peak as a function of prior polymer concentration at solution-crystallization.

amorphous layers separately. Each thickness of dark and bright layers, corresponding to amorphous and crystalline region, respectively, was measured on a number of TEM images for these samples. Approximately, 500 lamellae were randomly selected and evaluated for each sample. The resultant distribution curves were also plotted in Fig. 2. Both crystal and amorphous thickness distribution curves have their individual maximum peak tops, whose positions were independent of prior polymer concentration. Also, concerning the shape of the distribution curve, each set of crystalline or amorphous layers for these samples almost overlap. These results show that the stacking periodicity of crystalline/amorphous layers as well as their layer thickness of both phases lie in the same level for these samples.

For comparison with the above detailed evaluation of crystalline and amorphous layer thickness, the accurate long period value was determined by SAXS measurements using imaging plate system. As revealed in Fig. 1(B) and (D), SAXS patterns of solution-crystallized mats showed lamellar orientation parallel to the mat surface. Therefore, scattering diagram was reduced along the vertical direction in imaging plate patterns recorded for these series of samples solution-crystallized from different prior polymer concentration. Their SAXS profiles are compared in Fig. 3. The long periods lie in the constant position around 0.78°, independent of prior polymer concentration. However, the scattering peak intensity gradually grow sharper with increasing prior polymer concentration. Such a peak sharpness was evaluated by integral width of scattering profile. Here, background was estimated as the scattering profile on the horizontal scans for each sample, and subtracted from vertical profiles. The peak density thus obtained was plotted with long period value as a function of prior polymer concentration in Fig. 4. Long period value always locate around 11.5 nm, in contrast, the integral width value rapidly decreases with increasing prior polymer concentration at solution-crystallization. These characteristics on scattering profile strike morphological difference among the series of samples. It should be noted that both periodicity and orientation of lamellae are unchanged among them. Another possible explanation of such a difference of scattering intensity focuses on crystal/amorphous two-phase system. Recent SAXS analysis [21] shows that sample crystallinity or difference between electron densities in crystalline/amorphous phases significantly affect the scattering invariant obtained. In the case of crystallinity variety of the samples, WAXD analysis gave a constant value around 70% (see Fig. 5), which agrees well with the ratio of crystalline layer thickness to the total long period estimated by TEM layer thickness distribution measurements, as shown in Fig. 2.

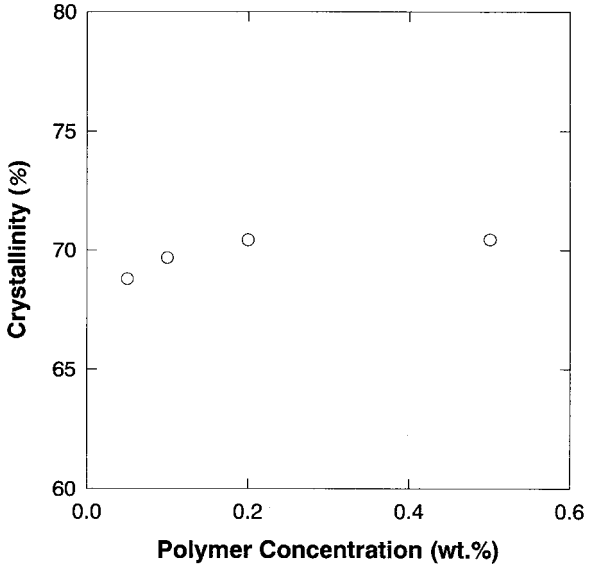

Fig. 5. Crystallinity estimated from WAXD patterns for the series of the solution-crystallized UHMW-PE mats.

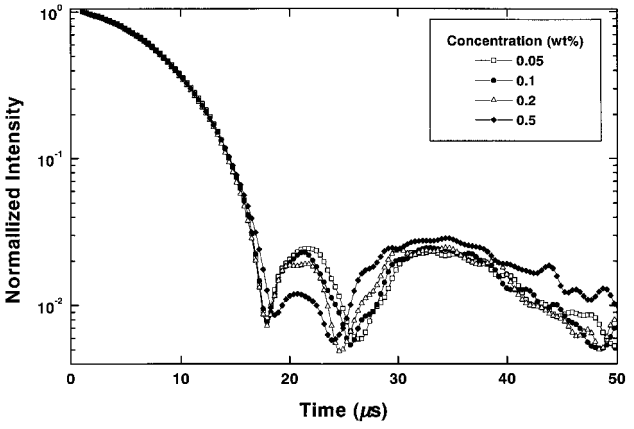

Fig. 6. A comparison of ^{1}H-NMR FID profiles between different prior polymer concentrations.

Such a constant crystallinity was similarly obtained from NMR analysis, which will be discussed later. This fact suggests that the origin of intensity difference among SAXS profiles could be ascribed to the difference in electron density between crystalline and amorphous phases. Here, the WAXD patterns for all samples showed usual lattice spacings giving constant lattice parameters. Thus, the electron density of crystalline phase should be unchanged. A survived assignment for the trend of SAXS profile intensity is an increase of electron density in amorphous layers with decreasing prior polymer concentration.

Another possible explanation for the variation of SAXS intensity might be the decrease of the crystalline disorder with increasing prior polymer concentration, assuming the constant amorphous density for all samples. Nevertheless, the results obtained did not agree with the same. The integral width of (002) reflection peak increases from 0.75 (0.05 wt%) to 0.83° (0.5 wt%), suggesting the increase of crystalline disorder when the constant crystal thickness is estimated from the observed constant crystallinity and lamellar thickness for the series of prior polymer concentration. Thus, the difference of amorphous density should still be considered for interpretation of the SAXS intensity trend observed here.

3.2. Chain relaxation behavior

Such a difference of amorphous characteristic, which could be detectable as a variety of SAXS profile shown in Fig. 3, was also accountable by NMR relaxation analysis. Fig. 6 compares the multiplied FIDs for the series of solution-crystallized mats prepared from different prior polymer concentrations. Here, to represent the magnetization intensity in logarithm scale, the negative beating drop observed was folded back to its positive side, which nominally gives an upward peak around 21 μs between two troughs. Such an up-field back-folding gradually drops downward with increasing prior polymer concentration. Also, it seems that the position of one of the troughs around 25 μs shifts to the longer time side with increasing prior polymer concentration. In contrast, the position of another trough around 19 μs is always located at the same point.

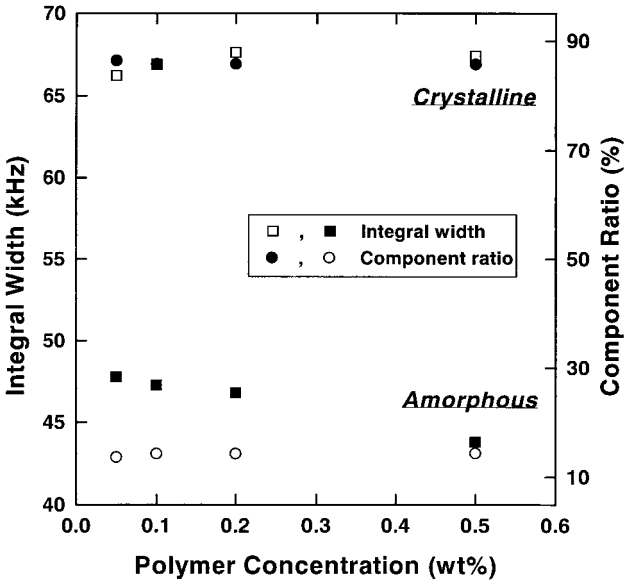

Fig. 7. Separated ^{1}H-NMR characteristics for crystalline and amorphous relaxations as a function of prior polymer concentration.

For decomposition of these FID profiles into crystalline and amorphous phases, which is also assumed on SAXS analyzing above, Gaussian/sine and Weibullian functions were applied for crystalline and amorphous chain relaxations, respectively. Detailed definition of these FID functions was described elsewhere [10]. These different functional decays could be compared in their Fourier-transformed formulas because they give individual single peak profile. Both area and width of these peaks transformed in frequency scale were compared within crystalline and amorphous phases. Sample crystallinity could be defined as a ratio of the crystalline area to that of total spectrum. Higher integral width represents shorter relaxation time corresponding to the hindered molecular motion. These two characteristics for relaxation in crystalline and amorphous phases were plotted in Fig. 7. The crystallinity obtained lies around 86%, independent of prior polymer concentration. Such a constant level of crystallinity is well coincident with the WAXD measurements results shown in Fig. 4. As for integral width, crystalline component brings a constant value around 67 kHz, in contrast, the amorphous one exhibits gradual decreasing with increasing prior polymer concentration. This trend of amorphous relaxation exhibits the restricted molecular motion in amorphous phase for a lower prior polymer concentration system.

Here, return to the changes of FID beat shape among the series of prior polymer concentration samples, as shown in Fig. 6. The unchanged position of the first trough around 19 μs, which is independent of prior polymer concentration, means the constant level of crystalline relaxation. The position of the second trough near 25 μs is significantly influenced by slope of amorphous relaxation decay. Shorter

relaxation time in the amorphous phase brings rapid decreasing FID, which emphasizes crystalline beating at the lower prior polymer concentration. In the present case, the series of samples have a same level of crystalline relaxation time and crystallinity, thus, the lower integral width of amorphous region gives gentle slope near beat, leading to the shift of the reversing point at the second trough to the longer time side.

Finally, observed results in TEM, X-ray and ^{1}H-NMR measurements could be summarized, focusing on difference in the amorphous chain characteristics for the series of solution-crystallized sample. The electron density in amorphous phases gradually increases with decreasing prior polymer concentration, as revealed from SAXS results. It was found that spin–spin relaxation time for amorphous phase increased similarly, based on ^{1}H-NMR analysis. In contrast, the component ratio of amorphous phases exhibits a constant value around 15%. A combination of these data clarifies that the amorphous molecular characteristics are quite different among the samples prepared from a variety of prior polymer concentrations. The less entangled state is kept for the sample solution-crystallized from prior lower polymer concentration, which induces the restricted molecular motion in amorphous phase, due to the formation of tie chains connecting crystalline layers through amorphous ones. Prior higher entangled state gives relaxed amorphous chains, compared to that for the former.

4. Conclusions

Morphological and relaxation characteristics of amorphous phase sandwiched between crystalline layers in solution-crystallized UHMW-PE samples are significantly affected by their prior polymer concentration at preparation. For samples crystallized from the dilute solution, the isolation of the chains is retained even in the solid state, which leads to the formation of less entangled amorphous molecules tying crystalline layers. Higher polymer concentration at solution preparation gave entangled amorphous state. These outlines were supported from TEM, X-ray and NMR results. The difference of electron density between crystalline and amorphous layers, which were alternatively stacked in the sample mat thickness, was emphasized by the higher polymer concentration at solution-crystallization, as revealed by SAXS peak intensity change. Also, ^{1}H-NMR relaxation behaviors showed that the accelerated amorphous chain motion for such a higher prior polymer concentration. In contrast, the similar features of crystalline phase, including crystallinity, lamellar thickness and crystalline molecular mobility, were confirmed for these series of samples solution-crystallized at different prior polymer concentrations. These results indicate that the amorphous molecular characteristics might be controlled by crystallization conditions. Interconnection of crystalline/amorphous layers in such stacked lamellar morphologies could be enhanced by less entangled state at the lowest polymer concentration. Such a cooperative relaxation in crystalline and amorphous components realized a role of tie molecules between crystalline/amorphous phases.

Acknowledgements

The original inspiration of entanglement concept in this paper was developed through a discussion with late Prof. Roger S. Porter at the University of Massachusetts at the time one of the authors (H.U.) joined his research group. The authors would like to express their deepest thanks for a number of his valuable suggestions on this subject.

References

[1] Porter RS, Johnson JF. J Appl Polym Sci 1960;3:1944.
[2] Porter RS, Johnson JF. Chem Rev 1966;66:1.
[3] Smith P, Lemstra PJ, Booij HC. J Polym Sci, Polym Phys Ed 1981;19:877.
[4] Smook J, Vos GJH, Doppert HL. J Appl Polym Sci 1990;41:105.
[5] Kanamoto T, Tsuruta A, Tanaka K, Takeda M, Porter RS. Macromolecules 1988;21:470.
[6] Sakurada I, Ito T, Nakamae K. J Polym Sci, Part C 1966;15:75.
[7] Higgins JS, Stein RS. J Appl Crystallogr 1978;11:346.
[8] Hadziioannou G, Wang LH, Stein RS, Porter RS. Macromolecules 1982;15:880.
[9] Sasaki S, Tashiro K, Goze N, Imanishi K, Izuchi M, Kobayashi M, et al. Polymer J 1999;31:677.
[10] Uehara H, Yamanobe T, Komoto T. Macromolecules 2000;33:4861.
[11] McCall DW, Douglass DC, Anderson EW. J Polym Sci 1962;59:301.
[12] Folland R, Charlesby A. J Polym Sci, Polym Lett Ed 1978;16:339.
[13] Folland R, Charlesby A. Eur Polym J 1979;15:953.
[14] Voigt G, Kimmich R. Polymer 1980;21:1001.
[15] Koch H, Bachus R, Kimmich R. Polymer 1980;21:1009.
[16] Kimmich R, Koch H. Colloid Polym Sci 1980;258:261.
[17] Kamel I, Charlesby A. J Polym Sci, Polym Lett Ed 1981;19:803.
[18] Cohen-Addan JP, Dupeyre R. Polymer 1983;24:400.
[19] Brereton MG, Ward IM, Boden N, Wright P. Macromolecules 1991;24:2068.
[20] Cohen-Addan JP, Feio G, Peguy A. Polym Commun 1987;28:252.
[21] Spells SJ, Hill M. J Polym 1991;32:2716.